Yang *et al. Journal of Neuroinflammation* (2024) 21:218
https://doi.org/10.1186/s12974-024-03204-6

Journal of Neuroinflammation

RESEARCH Open Access

Tyrosine phosphorylation and palmitoylation of TRPV2 ion channel tune microglial beta-amyloid peptide phagocytosis

Shaobin Yang[1*], Yaqin Du[1], Yanhong Li[1], Qi Tang[1], Yimeng Zhang[1] and Xiaoqian Zhao[1]

Abstract

Alzheimer's disease (AD) is the leading form of dementia, characterized by the accumulation and aggregation of amyloid in brain. Transient receptor potential vanilloid 2 (TRPV2) is an ion channel involved in diverse physiopathological processes, including microglial phagocytosis. Previous studies suggested that cannabidiol (CBD), an activator of TRPV2, improves microglial amyloid-β (Aβ) phagocytosis by TRPV2 modulation. However, the molecular mechanism of TRPV2 in microglial Aβ phagocytosis remains unknown. In this study, we aimed to investigate the involvement of TRPV2 channel in microglial Aβ phagocytosis and the underlying mechanisms. Utilizing human datasets, mouse primary neuron and microglia cultures, and AD model mice, to evaluate TRPV2 expression and microglial Aβ phagocytosis in both in vivo and in vitro. TRPV2 was expressed in cortex, hippocampus, and microglia.Cannabidiol (CBD) could activate and sensitize TRPV2 channel. Short-term CBD (1 week) injection intraperitoneally (i.p.) reduced the expression of neuroinflammation and microglial phagocytic receptors, but long-term CBD (3 week) administration (i.p.) induced neuroinflammation and suppressed the expression of microglial phagocytic receptors in APP/PS1 mice. Furthermore, the hyper-sensitivity of TRPV2 channel was mediated by tyrosine phosphorylation at the molecular sites Tyr(338), Tyr(466), and Tyr(520) by protein tyrosine kinase JAK1, and these sites mutation reduced the microglial Aβ phagocytosis partially dependence on its localization. While TRPV2 was palmitoylated at Cys 277 site and blocking TRPV2 palmitoylation improved microglial Aβ phagocytosis. Moreover, it was demonstrated that TRPV2 palmitoylation was dynamically regulated by ZDHHC21. Overall, our findings elucidated the intricate interplay between TRPV2 channel regulated by tyrosine phosphorylation/dephosphorylation and cysteine palmitoylation/depalmitoylation, which had divergent effects on microglial Aβ phagocytosis. These findings provide valuable insights into the underlying mechanisms linking microglial phagocytosis and TRPV2 sensitivity, and offer potential therapeutic strategies for managing AD.

Keywords Alzheimer's disease, Transient receptor potential vanilloid family type 2, Phagocytosis, Microglia, Phosphorylation

*Correspondence:
Shaobin Yang
yangshaobin@nwnu.edu.cn
[1]College of Life Sciences, Northwest Normal University, Lanzhou, Gansu 730070, China

Introduction

Alzheimer's disease (AD) is the most common form of dementia, it is characterized by a progressive deterioration of memory and cognitive function [1, 2]. Currently, AD affects more than 50 million individuals worldwide, and the number is reaching to triple within the next four decades [3]. AD is primarily associated with the formation of amyloid plaques, which is caused by the accumulation and aggregation of amyloid-β (Aβ) in the brain [4]. Amyloid plaques lead to neuronal damage, neuroinflammation, and disruption of synaptic function [5, 6]. Microglia play a pivotal role in preventing Aβ accumulation through phagocytosis-mediated clearance in central nervous system (CNS), triggering receptor expressed on myeloid cells 2 (Trem2) and TAM receptors (Axl and Mer) facilitating microglial recognition and engulfment of amyloid plaques [7, 8]. Therefore, it is crucial to inhibit the synthesis, accumulation, and aggregation of Aβ for the prevention of AD. The transient receptor potential vanilloid family type 2 (TRPV2) is associated with the risk of AD and mild cognitive impairment [9]. TRPV2, a Ca^{2+}-permeable non-selective cation channel, is widely expressed in most organs, and plays significant roles in axon outgrowth, osmotic- or mechanosensation, pro-inflammatory processes, and oncogenesis [10–12]. Furthermore, TRPV2 plays a crucial for phagocytosis in macrophages and microglia [13]. However, due to the absence of specific modulators, endogenous modulation of TRPV2 remains largely unexplored, making it difficult to pinpoint its exact TRPV2 molecular function [14]. Cannabidiol (CBD), a non-psychotropic compound, exhibits neuroprotective and anti-inflammatory properties in neurons via cannabinoid receptors. CBD reverses object recognition deficits and enhances the hippocampal immune response and autophagy in AD model mice [15, 16]. Similarly, CBD induces autophagy and improves neuronal health associated with SIRT1 mediated longevity in C. elegans [17]. CBD acts as a non-specific exogenous activator for TRPV2, showing much higher apparent affinity than other agonists [18, 19]. Recently, our study found that CBD improves microglial Aβ phagocytosis by modulation by TRPV2 [20]. Nevertheless, TRPV2 demonstrates varied effects on microglial phagocytosis. Under oxygen-glucose deprivation (OGD), CBD boosts TRPV2 expression but diminishes microglial phagocytosis [21]. Thus, it is essential to study the impact of CBD mediated TRPV2 modulation on microglial Aβ phagocytosis in AD mice. TRPV2 is primarily located on the endoplasmic reticulum membrane [22]. However, when microglia are activated by nitric oxide, TRPV2's regulation and migration from the endoplasmic reticulum to the plasma membrane along with the enhancement of its phagocytic function, depend on phosphoinositide 3-kinase signaling pathways (PI3Ks) [23, 24]. Recently, the oxidation of TRPV2 on methionine residues was discovered to activate and sensitize the channel [25]. Moreover, protein tyrosine phosphatase non-receptor type 1 (PTPN1) mediates TRPV2 dephosphorylation, and inhibiting JAK1 reduces TRPV2 channel activity and diminishes macrophage phagocytic ability [26]. Dynamic protein S-palmitoylation also contributes to protein transport and functional localization by increasing protein hydrophobicity [27, 28]. Palmitoylation regulates cellular distribution of and transmembrane Ca^{2+} flux through TrpM7 [29]. TRPML1 is palmitoylated following histamine stimulation of acid secretion [30]. TRPC5 channel instability induced by depalmitoylation protects striatal neurons against oxidative stress in Huntington's disease [31]. Intriguingly, palmproteomics suggests that TRPV2 may undergo palmitoylation. Meanwhile, the physiological and pathological roles of TRPV2 in microglial phagocytic ability is required to comprehensively understand. In this study, the function of TRPV2 channel in microglial Aβ phagocytosis and the underlying mechanisms were examined. It was found that microglial TRPV2 channel is regulated by tyrosine phosphorylation/dephosphorylation and cysteine palmitoylation/depalmitoylation, exhibits divergent effects on microglial Aβ phagocytosis.

Results

Short-term CBD injection (i.p.) reduced the expression of neuroinflammation and microglial phagocytic receptors via TRPV2 channel

First, the TRPV2 expression in the brain zone of wild-type (WT) mice was determined, the TRPV2 protein expression was shown in the cortex, telencephalon, and hippocampus (Fig. S1A). When characterizing the expression pattern of TRPV2 in the brain, the TRPV2 protein expression in microglia was significantly higher than the neuronal or astrocytic expression (Fig. S1B). To further understand the impact of AD on TRPV2 expression in brain, we analyzed cell-type specific data from human brain cortical tissue based on the τ enrichment score [32]. Results highlighted microglia exhibiting the highest TRPV2 levels among the TRPV family (Fig. S1C-D). Bioinformatics analysis unveiled the conservation of the amino acid sequence of the TRPV2 channel across humans, mice, and rats (Fig. S1E). Using AlphaFold2, it was determined that full-length mouse TRPV2 forms a tetrameric protein, and CBD could bind to mTRPV2 through a hydrophobic pocket located between the S5 and S6 helices (Fig. 1A). We then asked whether CBD exerts beneficial effects on TRPV2/Akt pathway in APP/PS1 mice. We observed a significant increase in the TRPV2 protein levels in the cortex of both WT and APP/PS1 mice after CBD was injected (i.p.) for 1 week (Fig. 1B and C). The phosphorylation level of Akt at

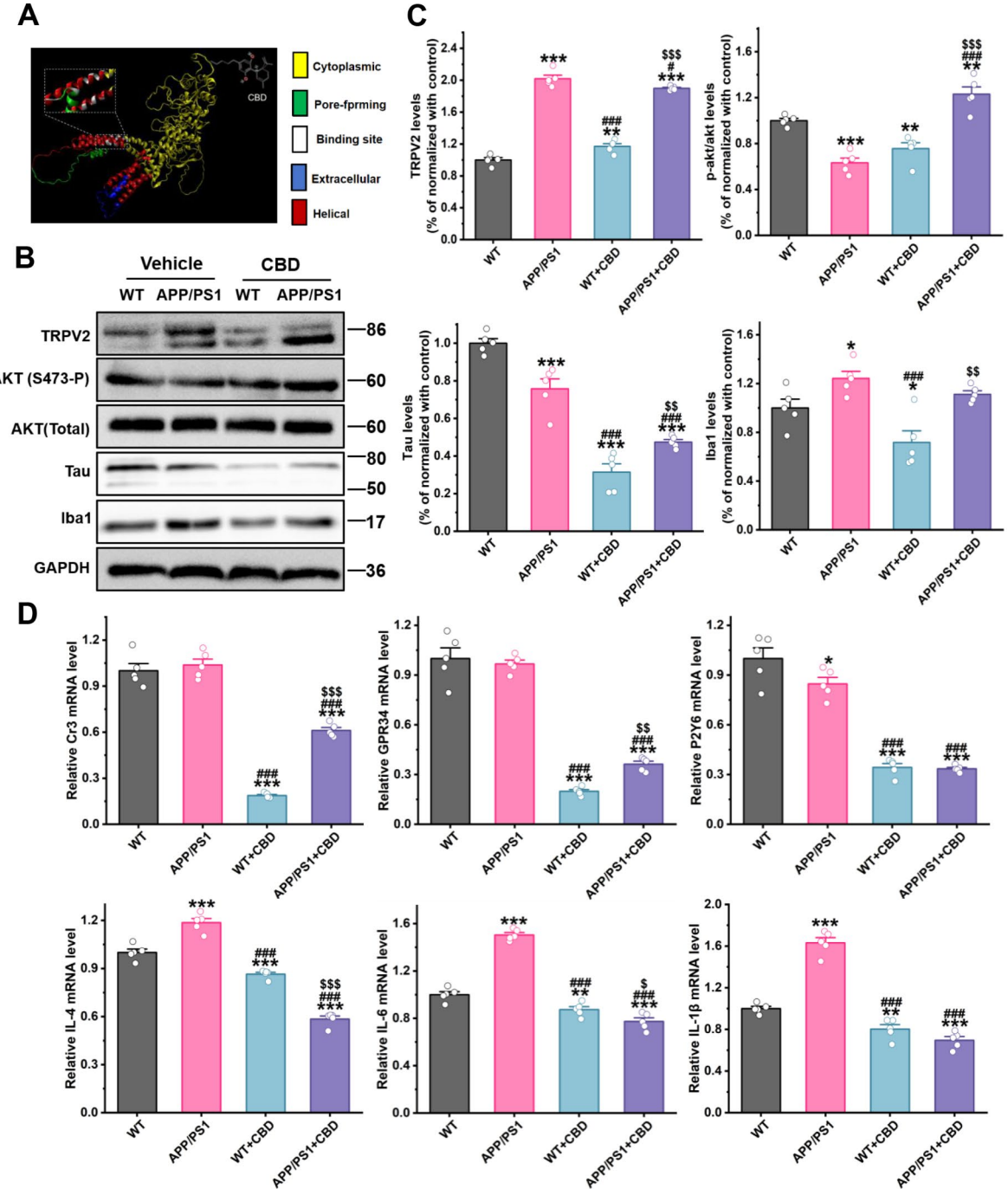

Fig. 1 Short-term CBD treatment modulated mRNA and protein expression in the cortex of APP/PS1 mice. **(A)** A schematic diagram depicting the binding of CBD to TRPV2 in mice is shown, the binding site represented in white. **(B)** WT and APP/PS1 mice were treated with or without CBD (10 mg/kg/d for 1 week), protein expression was determined by immunoblot analysis with the depicted antibodies. **(C)** Band densitometry quantification normalized to GAPDH levels or Akt phosphorylated and Akt total protein levels are shown. **(D)** mRNA levels were determined by RT-qPCR. The data are presented as the mean ± SEM ($n = 5$ per group) independent experiments conducted in triplicate. $^{*}p < 0.05$, $^{**}p < 0.01$, and $^{***}p < 0.001$ are compared to WT treated by saline, $^{\#}p < 0.05$, $^{\#\#}p < 0.01$, and $^{\#\#\#}p < 0.001$ compared to APP/PS1 mice treated by saline, $^{\$}p < 0.05$, $^{\$\$}p < 0.01$, and $^{\$\$\$}p < 0.001$ are compared to WT treated by CBD, as obtained by one-way analysis of variance (ANOVA). Vehicle: saline. WT: wild type + saline, APP/PS1: APP/PS1 + saline

Ser473 was significantly increased in the cortex of APP/PS1 mice by CBD treatment (Fig. 1B and C). Notably, the protein level of Tau was weakly reduced by CBD treatment, and ionized calcium binding adaptor molecule 1 (Iba1) was a slight reduction in the cortex of APP/PS1 mice, but there was no statistical difference (Fig. 1B and C). To investigate the effects of CBD on neuroinflammation and microglial phagocytic receptors in AD, we

performed qRT-PCR to measure the mRNA expression levels of various cellular cytokines and phagocytic receptors, including G protein-coupled receptor 34 (GPR34), complement receptor 3 (CR3), purinergic receptor P2Y6 (P2Y6), interleukin-1β (IL-1β), IL-6, and IL-4. CBD treatment significantly decreased the cortical mRNA expression levels of Cr3, GPR34, P2Y6, IL-4, IL-6, and IL-1β compared with saline group in APP/PS1 mice (Fig. 1D). These data demonstrate that short-term CBD treatment significantly decreases chronic neuroinflammation and microglial phagocytic receptors in AD mice.

Long-term CBD injection (i.p.) aggravated amyloid plaques without altering neuronal death in APP/PS1 mice

We then explored whether long-term CBD treatment offers beneficial effects in mitigating neuronal apoptosis and Aβ pathology, two significant features of AD. To examine CBD's on neuronal activity, we assessed neuronal viability by quantifying NeuN-positive neurons in mice. Following prolonged CBD injection (i.p.) in APP/PS1 mice, as illustrated in Fig. 2A, no apparent differences in NeuN staining were observed among the four groups (WT + saline vs. APP/PS1 + saline vs. WT + CBD vs. APP/PS1 + CBD) in the medial prefrontal cortex (mPFC) and the hippocampal dentate gyrus (DG) region (Fig. 2C-D). Furthermore, primary cortical neurons were employed to measure the percentage of apoptotic cells. As expected, exposure to Aβ oligomers led to a notable increase in apoptotic cell percentage. Nonetheless, CBD treatment effectively rescued the neuronal death induced by Aβ oligomers (Fig. S2).

To confirm CBD's potential in addressing Aβ pathology in the AD brain, we utilized APP as a marker for protein expression in APP/PS1 mice. Our results indicated the absence of APP expression in WT mice, while the cortex and hippocampus of APP/PS1 mice exhibited APP presence (Fig. 3A and S3A). Interestingly, CBD administration led to an increase in APP protein expression in both the cortex and hippocampus of APP/PS1 mice (Fig. 3A and S3A). Aβ accumulation and aggregation result from an imbalance in Aβ production [33]. To further explore the effect of long-term CBD on amyloid burden in mice, brain sections were immunostained with an anti-Aβ antibody, and the number of Aβ plaques was quantified. Immunopositivity was completely absent in the cortex and hippocampus of WT mice (Fig. 2E). CBD significantly increased the number of Aβ- immunostained plaques in the cortex and hippocampus of APP/PS1 mice (Fig. 2F and G). These findings collectively suggest that long-term CBD injection activates TRPV2 channel and aggravates amyloid plaques, without altering neuronal apoptosis in APP/PS1 mice.

Overactivation of TRPV2 by CBD led to neuroinflammation and phagocytic dysfunction in APP/PS1 mice

Our previous study has demonstrated that CBD enhances Aβ phagocytosis in microglia via Akt signaling pathway mediated by TRPV2 [20]. However, we observed a notable increase in TRPV2 protein levels in the hippocampus and cortex following prolonged CBD treatment in APP/PS1 mice (Fig. 3A and S3A). The Akt phosphorylation at Ser473 significantly decreased in both WT and APP/PS1 mice after CBD administration. Surprisingly, the protein levels of Tau and Iba1 showed a marked increase in the hippocampus and cortex post-CBD treatment in WT and APP/PS1 mice, but Beta-site-APP Cleaving Enzyme (BACE) slightly increased in APP/PS1 + CBD compared to APP/PS1 + saline (Fig. 3A and S3A). These findings are intriguing given the prior evidence of CBD's promotion of microglial Aβ phagocytosis and clearance via TRPV2 activation [20]. We speculate that CBD-induced TRPV2 channel activation might contribute to microglial polarization and the release of inflammatory factors, potentially leading to impaired Aβ phagocytosis [20]. To further explore CBD's effects on microglial phagocytic capacity and inflammation in AD brain tissues, we conducted qRT-PCR to evaluate cytokine and phagocytic receptor levels in APP/PS1 mice. Our results revealed that CBD administration upregulated mRNA levels of Iba1, TRPV2, Triggering receptor expressed on myeloid cells 2 (Trem2), Cr3, as well as inflammatory factors IL-6, TNFα, and IL-1β in the hippocampus of APP/PS1 mice, CBD improved the mRNA expression of Iba1, Trem2, and P2Y6 in the hippocampus of WT mice (Fig. 3B). Furthermore, CBD treatment resulted in increased cortical mRNA levels of Iba1, P2Y6, and TNFα in APP/PS1 mice, CBD administration upregulated mRNA levels of Iba1, TRPV2, Trem2, Cr3, P2Y6 and IL-6 in the cortex of WT mice (Fig. S3B). Together, these findings suggest that CBD-induced overactivation of TRPV2 channel may contribute to neuroinflammation and impaired phagocytic function in APP/PS1 mice.

Hypersensitivity of TRPV2 channel by tyrosine dephosphorylation reduced microglial Aβ phagocytosis

To investigate the effects of TRPV2 overexpression on microglial phagocytosis, we introduced TRPV2 plasmids into microglia and treated them with FITC- conjugated Aβ. Our results indicated that while CBD treatment slightly enhanced microglial Aβ phagocytosis, there was a reduction in the uptake of FITC-Aβ42 and the internalized amount of FITC-Aβ42 following TRPV2 plasmid transfection, despite CBD increasing TRPV2 expression on the membrane (Fig. 4A, B, and E). Previous study has shown that JAK1 can enhance TRPV2 phosphorylation [26]. To investigate this, we employed ruxolitinib, a selective kinase inhibitor that blocks JAK signaling and

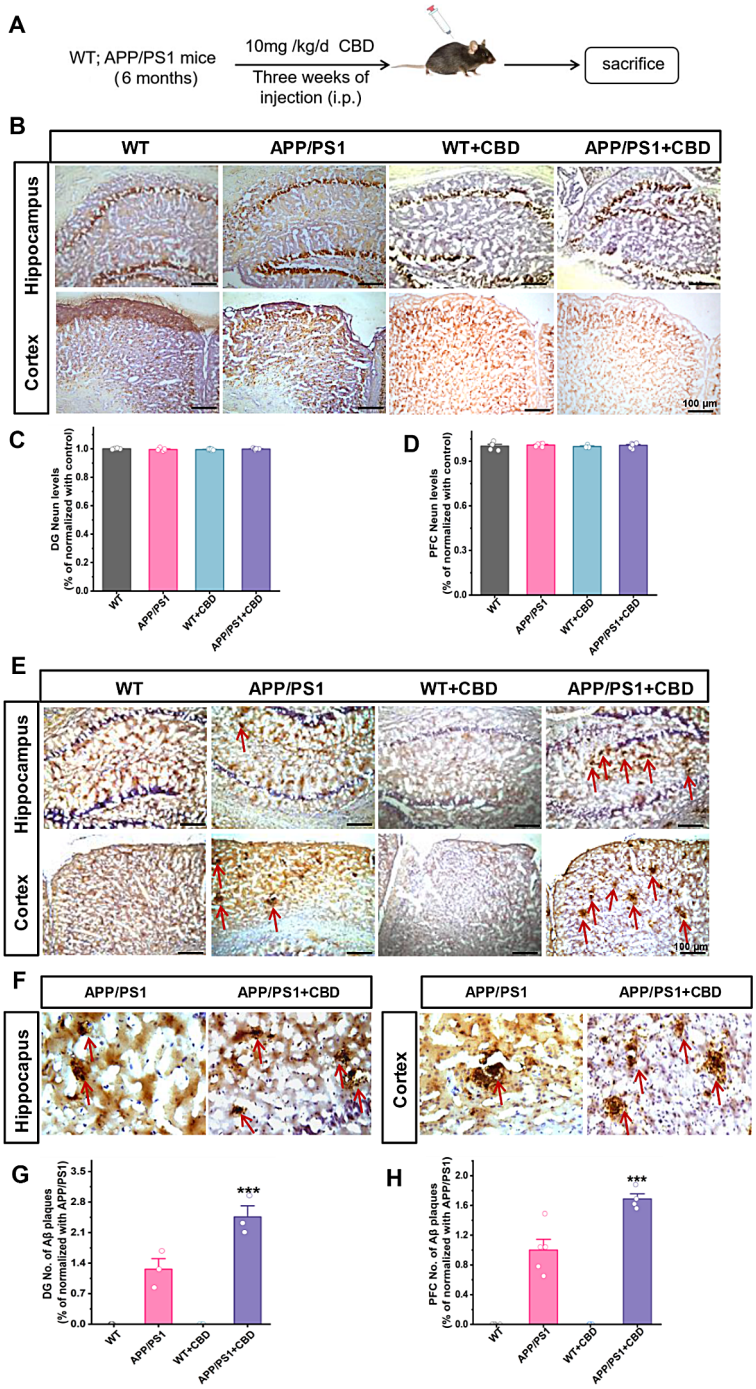

Fig. 2 Long-term CBD treatment did not affect the expression of NeuN but exacerbated amyloid plaques in APP/PS1 mice. **(A)** Schematic illustrations of the experiment and timeline. Immunohistochemical staining of brain sections obtained from WT and APP/PS1 mice after the last injection of saline or CBD (10 mg/kg/d for 21 days). **(B-D)** The numbers of cells in the medial prefrontal cortex (mPFC) and hippocampal dentate gyrus (DG) NeuN were quantified and are expressed as a percentage of WT controls with saline. **(E)** The amyloid plaques in the mPFC and DG were stained, and the numbers in the cortex **(F)** and **(G)** hippocampus were quantified and are expressed as a percentage of those in the WT controls treated with saline. The data are presented as the mean ± SEM at least of five different mice per group ($n = 10$) independent experiments conducted in triplicate. One-way ANOVA, followed by Post hoc Tukey's test for multiple comparisons, was used to analyze the data. $^{***}p < 0.001$ versus WT group. The scale bars = 100 μm–75 μm. WT: wild type + saline, APP/PS1: APP/PS1 + saline

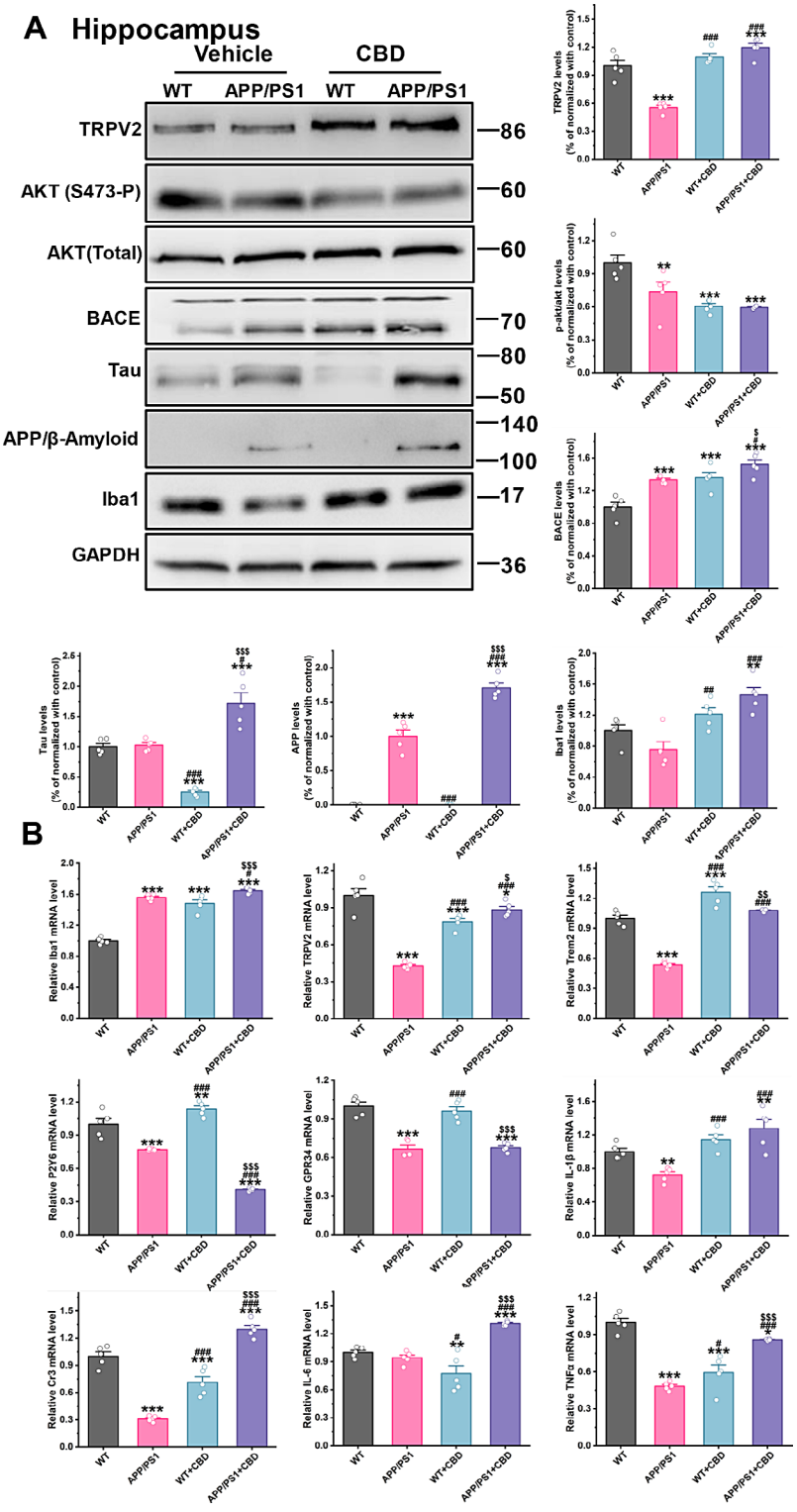

Fig. 3 Long-term CBD injection (i.p.) modulated mRNA and protein expression in the hippocampus of six-month-old APP/PS1 mice. WT and APP/PS1 mice were treated with or without CBD (10 mg/kg/d for 21 days), and **(A)** protein and **(B)** mRNA levels were determined by RT-qPCR and immunoblot. Protein extracts were obtained from the hippocampus and immunoblotted with the depicted antibodies, and GAPDH was used as a loading control. The data are presented as the mean ± SEM ($n = 5$ per group) independent experiments conducted in triplicate. $^{*}p < 0.05$, $^{**}p < 0.01$, and $^{***}p < 0.001$ are compared to WT treated with saline, $^{\#}p < 0.05$, $^{\#\#}p < 0.01$, and $^{\#\#\#}p < 0.001$ compared to APP/PS1 mice treated with saline, $^{\$}p < 0.05$, $^{\$\$}p < 0.01$, and $^{\$\$\$}p < 0.001$ are compared to WT treated with CBD, as obtained by one-way analysis of variance (ANOVA). WT: wild type; Vehicle: saline. APP/PS1: APP/PS1 + saline

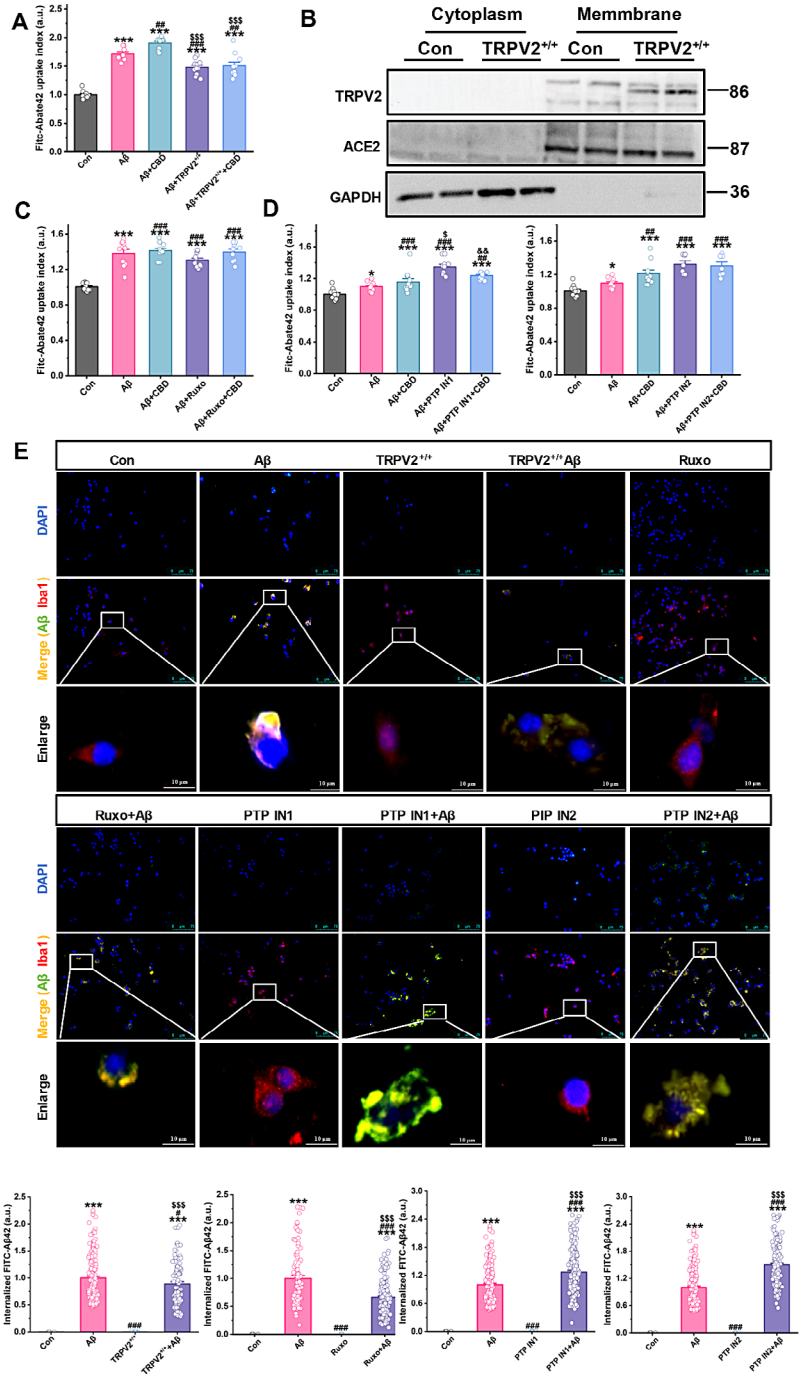

Fig. 4 Hyper-sensitivity of TRPV2 channels by tyrosine dephosphorylation reduced microglial Aβ phagocytosis. **(A)** Primary microglia were transfected with the TRPV2 pCMV-TRPV2-3FLAG-Neo plasmid for 48 h, and then treated with CBD for 24 h, FITC-Aβ42 (1 μg/ml) was added to the medium for another 24 h, and the FITC-Aβ42 uptake index was calculated based on the phagocytosis assay. **(B)** BV2 cells were transfected with the TRPV2 pCMV-TRPV2-3FLAG-Neo plasmid, cell cytosolic and membrane fractions were obtained and immunoblotted with the indicated antibodies, with GAPDH and ACE2 used as cytosolic and membrane markers, respectively. **(C-D)** Primary microglia were pre-added with Ruxo (ruxolitinib, 10 μM) 4 h, PTP IN 1 (protein tyrosine phosphatase (PTP) inhibitor 1, 0.5 μM), PTP IN 2 (protein tyrosine phosphatase (PTP) inhibitor 2, 0.5 μM) for 5 min, and treated with or without CBD for 24 h, FITC-Aβ42 (1 μg/ml) was added to the medium for another 24 h, FITC-Aβ42 uptake index was analyzed using the phagocytosis assay. **(E)** Primary microglia were plated at a density of 5×10^4 in poly-D-lysine-coated wells of 24-well plates containing DMEM supplemented with 10% FBS. Cells were transfected with TRPV2 pCMV-TRPV2-3FLAG-Neo plasmid for 48 h, or pretreated with Ruxo (ruxolitinib, 10 μM) 4 h, PTP IN 1 (0.5 μM), PTP IN 2 0.5 μM) for 5 min, FITC-Aβ42 (1 μg/ml) was added to the medium. Immunofluorescence analysis of microglial phagocytosis of FITC-Aβ42 was performed after allowing uptake for 24 h. $^{*}p < 0.05$, $^{**}p < 0.01$, and $^{***}p < 0.001$ are compared to control, $^{\#\#}p < 0.01$ and $^{\#\#\#}p < 0.001$ are compared to Aβ, $^{\$}p < 0.05$ and $^{\$\$\$}p < 0.001$ are compared to CBD + Aβ, $^{\&}p < 0.05$ is compared to CBD + PTP IN 1, as obtained by one-way analysis of variance (ANOVA). Con: DMSO

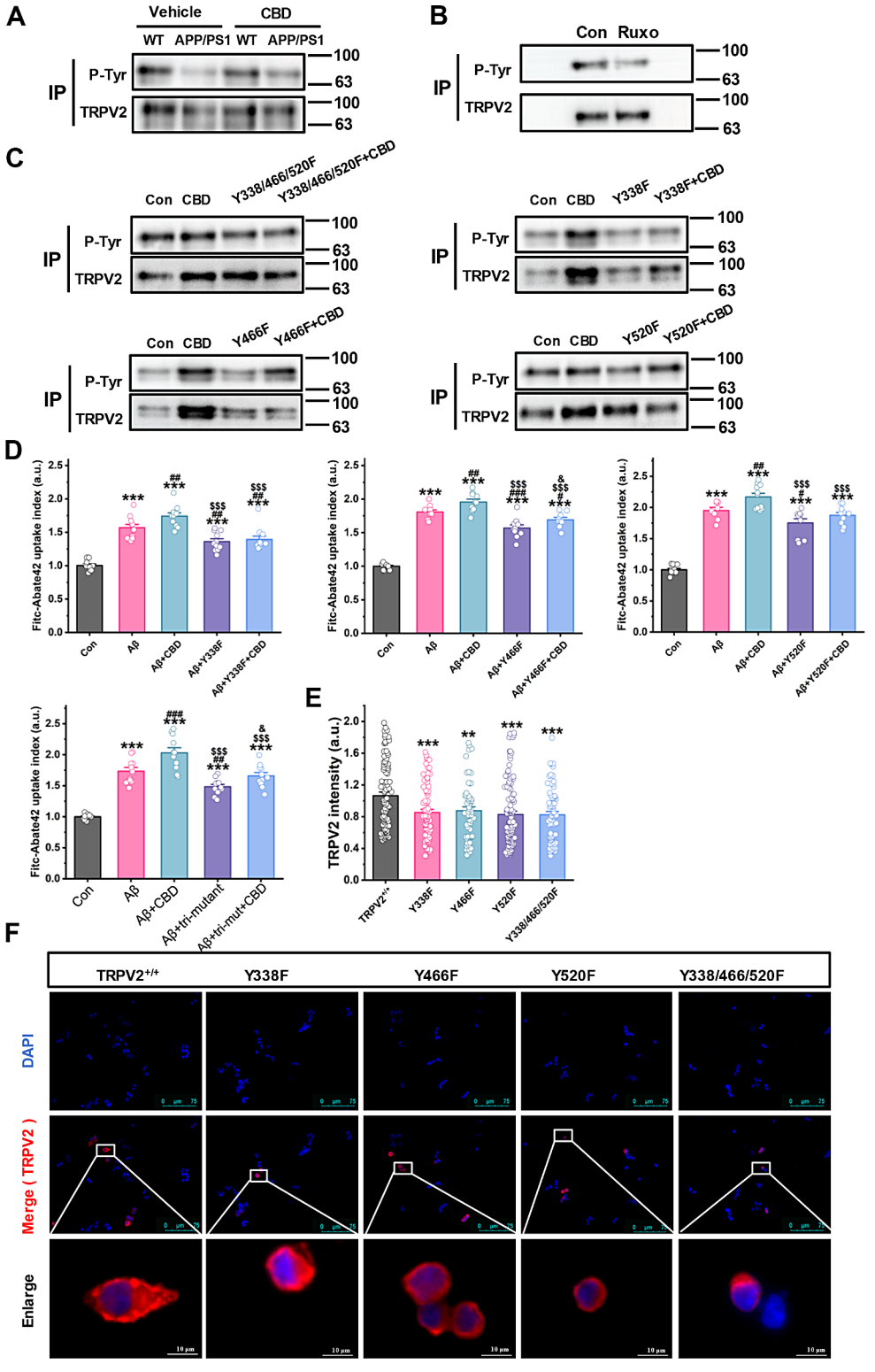

Fig. 5 (See legend on next page.)

transcriptional activation factor pathways [26]. The optimal time and dose of ruxolitinib were determined using the MTT assay (Fig. S4A). Microglia were then treated with ruxolitinib to assess their phagocytic ability. The results demonstrated that cotreatment with ruxolitinib and Aβ modestly reduced the capacity of microglia to uptake FITC-Aβ compared to the Aβ group (Fig. 4C). Moreover, immunocytochemistry analysis revealed a

(See figure on previous page.)

Fig. 5 JAK1 phosphorylated TRPV2 at the Y338, Y466, and Y520 molecular sites. **(A)** 6-months-APP/PS1 mice were treated with or without CBD (10 mg/kg/d for 21 days), **(B)** microglia cells were treatment with Ruxo (ruxolitinib, 10 μM) 4 h, and tyrosine phosphorylation of immunoprecipitated TRPV2 in cortical tissues or cells was determined by immunoblotting with an anti-phosphotyrosine antibody. Microglia or HEK293T cells were transfected with the TRPV2 pCMV-TRPV2-3FLAG-Neo, pCMV-TRPV2-Y338F-3FLAG-Neo, pCMV-TRPV2-Y466F-3FLAG-Neo, pCMV-TRPV2-Y520F-3FLAG-Neo, pCMV-TRPV2-Y338/466/520F-3FLAG-Neo plasmids for 48 h, and then after treatment with CBD for 24 h, FITC-Aβ42 (1 μg/ml) was added to the medium for 24 h. **(C)** Tyrosine phosphorylation of immunoprecipitated TRPV2 transiently transfected into HEK293T cells were determined by immunoblotting with an anti-phosphotyrosine antibody after treated with Ruxo (ruxolitinib, 10 μM) 4 h. **(D)** The FITC-Aβ42 uptake index was analyzed using the phagocytosis assay. **(E)** and **(F)** Primary microglia were plated at a density of 5×10^4 in poly-D-lysine-coated wells of 24-well plates containing DMEM supplemented with 10% FBS. Immunofluorescence analysis of microglial TRPV2 expression was determined. $^{**}p < 0.01$ and $^{***}p < 0.001$ compared to control or TRPV2$^{+/+}$, $^{\#}p < 0.05$, $^{\#\#}p < 0.01$ and $^{\#\#\#}p < 0.001$ compared to Aβ, $^{\$\$}p < 0.01$ and $^{\$\$\$}p < 0.001$ compared to CBD + Aβ, as obtained by one-way analysis of variance (ANOVA). Con: DMSO. tri-mutant or tri-mut: Y338/466/520F

significant decrease in the engulfment of FITC-Aβ42 peptides following cotreatment with ruxolitinib and Aβ (Fig. 4E).

Protein phosphorylation, a reversible post-translational modification is regulated by both kinases and phosphatases [26]. Protein tyrosine phosphatase (PTP) inhibitors were used to search for the phosphatases that mediated the dephosphorylation of TRPV2 [26]. PTP inhibitor 1 (2-bromo-4'-hydroxyacetophenone) and PTP inhibitor 2 (4-(bromoacetyl)anisole) are inhibitors for TRPV2 dephosphorylation, they could enhance the tyrosine phosphorylation level of TRPV2 [26]. The optimal time and dose of PTP inhibitors 1 and 2 were determined via MTT assay (Fig. S4B and C). We subsequently examined the impact of PTP-mediated dephosphorylation of TRPV2 on the microglial phagocytic ability. Treatment with PTP inhibitor 1 and PTP inhibitor 2 modestly increased the efficiency of FITC-Aβ uptake, while microglial phagocytic ability decreased upon co-treatment with CBD and PTP inhibitor 2 (Fig. 4D). Accordingly, compared to the Aβ42 group, the amount of internalized FITC-Aβ42 in the CBD and PTP inhibitor 2 or PTP inhibitor 1 co-treatment group was also higher (Fig. 4E). These findings indicate that tyrosine phosphorylation enhances TRPV2 sensitivity and improves microglial Aβ phagocytosis, which is regulated by phosphatase-mediated dephosphorylation.

JAK1 phosphorylated TRPV2 at the Y338, Y466, and Y520 molecular sites

We then investigated the molecular mechanism of TRPV2 channel regulated by tyrosine phosphorylation. We firstly determined the tyrosine phosphorylation level of TRPV2 in the AD brain through immunoprecipitation. Our findings indicated a decrease in TRPV2 tyrosine phosphorylation in the cortex of APP/PS1 mice, which was reversed by CBD treatment, while CBD treatment slightly enhanced total TRPV2 expression compared to control (Fig. 5A). Interestingly, ruxolitinib also reduced TRPV2 tyrosine phosphorylation in macroglia (Fig. 5B). JAK1 phosphorylates rat TRPV2 at sites Y335, Y471, and Y525 [26]. Using the conservation of TRPV2 sequence across species and the prediction of tyrosine phosphorylation sites in mouse TRPV2, we identified potential sites in mouse TRPV2. Transfecting TRPV2 plasmids containing TRPV2 Y338F, Y466F, Y520F, as well as a triple mutant TRPV2 plasmid (Y338/466/520F) into HEK293T cells, TRPV2 levels were downregulated at the Y520F, and tri-mutant sites, but not at the Y466F and Y338F sites upon CBD treatment (Fig. S5A). The tyrosine phosphorylation levels of immunoprecipitated TRPV2 protein decreased in cells expressing TRPV2 Y520F and TRPV2 (Y338/466/520F) plasmids. Interestingly, CBD treatment augmented TRPV2 channel sensitivity at the Y466F and Y520F sites, but not at the Y338F or the tri-mutant site (Fig. 5C).

To explore how mutations at these sites affect microglial Aβ phagocytosis, we transfected TRPV2 Y338F, Y466F, Y520F, and TRPV2 (Y338/466/520F) plasmids into microglia. This led to a modest reduction in microglial Aβ phagocytosis compared to Aβ+plasmid group, especial in TRPV2 Y338F, Y466F, and TRPV2 (Y338/466/520F) plasmids. CBD only improved microglial Aβ phagocytosis in the Y466F and TRPV2 (Y338/466/520F) plasmids, although the effect is not drastic (Fig. 5D). Moreover, fluorescence intensity surrounding microglia decreased after transfection with TRPV2 Y338F, Y466F, Y520F, and TRPV2 (Y338/466/520F) plasmids following 24 h FITC-Aβ treatment (Fig. S5B). TRPV2 typically relocates from the endoplasmic reticulum to the cell membrane upon activation, facilitating Aβ phagocytosis by microglia [24]. We examined whether mutations at these sites affect TRPV2 localization. Our findings revealed that transfection with the TRPV2 plasmid exhibited the highest fluorescence intensity and TRPV2 expression on the cell membrane (Fig. 5E-F). Conversely, transfection with TRPV2 Y338F, Y466F, Y520F, and TRPV2 (Y338/466/520F) plasmids not only decreased TRPV2 fluorescence intensity in microglia, but also reduced the levels of TRPV2 expression on the cell membrane (Fig. 5E-F and S6). These findings suggest that tyrosine phosphorylation sites, especially Y338 and Y520 of TRPV2 regulate microglial Aβ phagocytosis partially depend on its localization.

TRPV2 was palmitoylated at cysteine 277 site and reduced microglial Aβ phagocytosis

TRPV2 was identified as a potential palmitoylated protein based on palm-proteomics analysis. Employing an ABE assay on TRPV2 expressed in HEK293T cells, we found that TRPV2 is palmitoylated (Fig. 6A). We then assessed palmitoylation levels in the brain of AD mice. Results revealed elevated cortical levels in APP/PS1 mice following HAM treatment compared to WT mice, with CBD enhancing the palmitoylation levels in AD mice (Fig. S7A and B). Further investigation identified cysteine 277 as the specific site of palmitoylation on TRPV2 (Fig. 6B). To ascertain the impact of TRPV2 palmitoylation on microglial phagocytic ability, we evaluated the phagocytosis of FITC-Aβ and fluorescence intensity surrounding microglia after transfection with TRPV2 and TRPV2 C277A plasmids. The TRPV2 C277A group exhibited slightly higher fluorescence intensity of internalized Aβ surrounding microglia compared to the Aβ group (Fig. 6C). While transfection with the TRPV2 C277A plasmid did not alter microglial Aβ phagocytosis induced by CBD (Fig. 6D). Examining TRPV2 localization, upon transfection of TRPV2 and TRPV2 C277A plasmids into HEK293T cells revealed reduced the membrane expression with the C277A plasmid (Fig. 6E). Interestingly, no significant difference in TRPV2 fluorescence intensity on the cell membrane was observed between the mutation and overexpression groups (Fig. 6F). Palmitoylation is catalyzed by a family of ZDHHC domain-containing S-acyltransferases [34]. Substrate specificity analysis viapalm-proteomics, suggested ZDHHC21 as a potential enzyme involved in TRPV2 palmitoylation. To validate this, we expressed a hemagglutinin (HA)-tagged ZDHHC21 enzyme in HEK293T cells, followed by analysis of TRPV2 palmitoylation by ABE assay. Results indicated an increase in TRPV2 palmitoylation level upon ZDHHC21expression (Fig. S7C).

In this study, we explored the effects of 2-Bromopalmitate (2-BP), a compound inhibiting palmitoylation by targeting palmitoyltransferase on microglia and their ability to phagocytose FITC-Aβ [35]. Initially, we determined the optimal time and concentration of 2-BP (Fig. S7D). Microglia were treated with 2-BP and subsequently exposed to FITC-Aβ for 24 h. Interestingly, we found that 2-BP treatment enhanced microglial phagocytosis of Aβ, and this phagocytic ability was further boosted when CBD and Aβ were co-administered (Fig. S7E). To explore the role of TRPV2 palmitoylation in microglia response to Aβ, we examined TRPV2 expression in microglia treated with 2-BP and Aβ. Our results indicated that co-treatment with 2-BP and Aβ led to time-dependent decrease in TRPV2 expression. Importantly, this treatment did not affect the phosphorylation of CaMKIIα/δ at Thr286 (Fig. S7F). Together, these findings suggest that TRPV2 palmitoylation negatively regulates microglial phagocytosis of Aβ.

Discussion

TRPV2 is identified as a promising therapeutic target in AD for its role in regulating microglial Aβ phagocytosis. Our study utilized cellular and animal models to investigate the role of TRPV2 channel in microglial Aβ phagocytosis, we found that TRPV2 channel was modulated by tyrosine phosphorylation/dephosphorylation and cysteine palmitoylation/depalmitoylation, exhibited opposing impacts on microglial Aβ phagocytosis. These findings illuminate the underlying connections between microglial phagocytosis and TRPV2 sensitivity.

Our data demonstrated that TRPV2 protein expression was expressed in the hippocampus and cortex. Among TRPV family members, TRPV2 was expressed at the highest level in microglia. Notably, our previous study showed that the protein level of TRPV2 is greater in microglia than in neurons [20]. Considering the pivotal role of microglia in AD pathophysiology through Aβ phagocytosis and inflammatory cytokine secretion, these results strongly indicate that microglial TRPV2 could hold significant implications for AD development [9]. TRPV2 has been proposed as a potential target for various stimuli, including redox processes, temperature changes, and membrane depolarization, all known to activate TRPV2 channels in rodents [36]. CBD, a natural compound with neuroprotective, anti-inflammatory, and antioxidant properties, has emerged as a promising therapeutic candidate for AD [37–39]. CBD exhibits its neuroprotective and anti-inflammatory properties in neurons via cannabinoid receptors [15]. CBD reverses object recognition deficits and enhances the hippocampal immune response and autophagy in AD model mice [16]. Similarly, CBD induces autophagy and improves neuronal health associated with SIRT1 mediated longevity in C. elegans [17]. Our findings also found that CBD could effectively rescue neuronal death caused by Aβ both in APP/PS1 mice and primary cortical neurons, suggesting CBD exhibits neuroprotective in neurons via cannabinoid receptors. CBD demonstrates notably higher apparent affinity for TRPV2 compared to other agonists [18, 19]. CBD interacts with TRPV2 via a hydrophobic pocket situated between the S5 and S6 helices in the PH domain, this direct interaction between CBD and TRPV2 is believed to underlie the modulation of TRPV2 activity [40, 41].

CBD significantly enhances microglial phagocytic capacity by activating TRPV2 channel, thereby facilitating the clearance of Aβ within microglia [20]. When co-administered with Aβ42, treatment with 2-APB (a TRPV2 agonist) or capsaicin (a TRPV1 agonist) markedly enhances the phagocytic capacity of microglia [20].

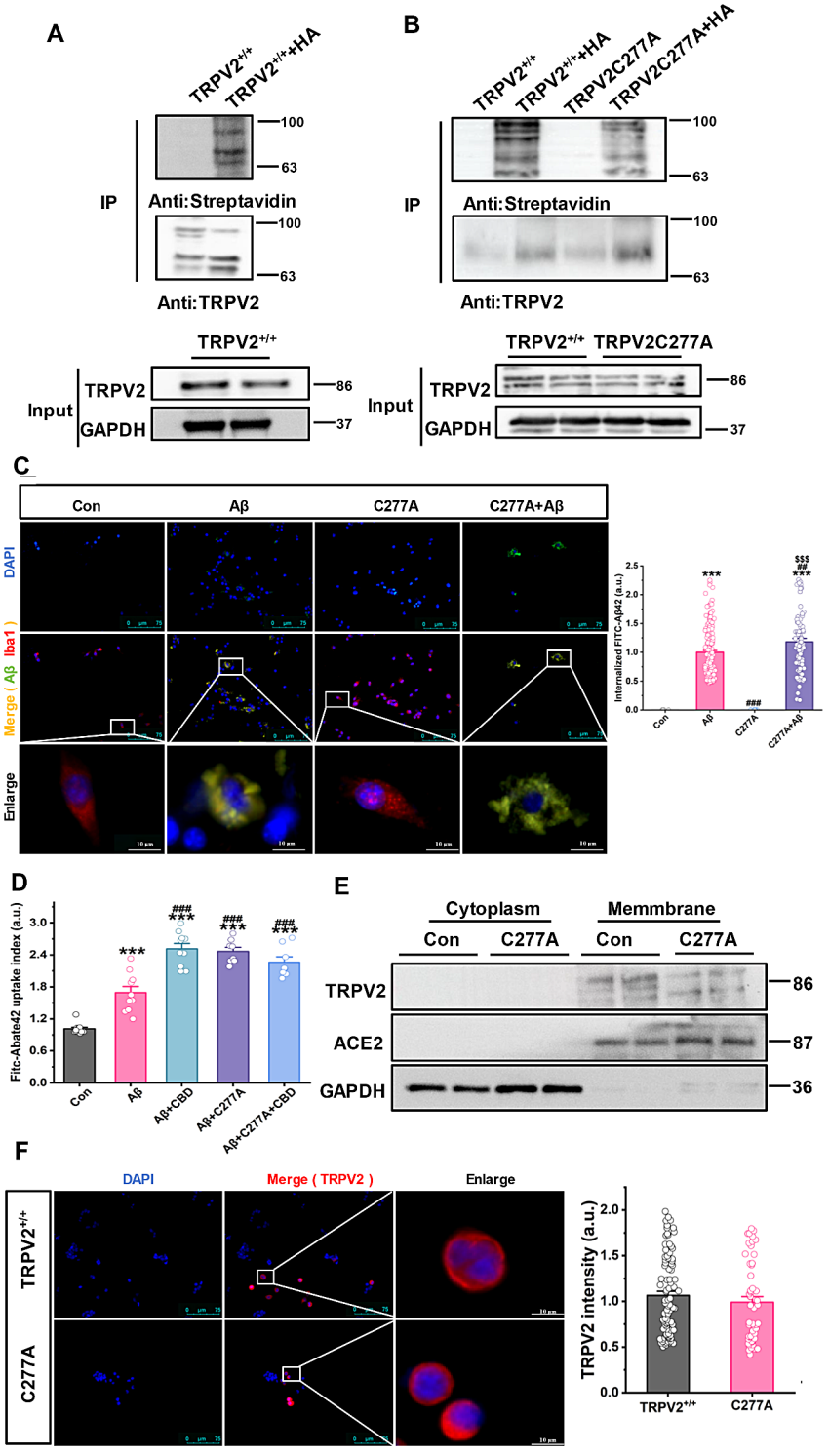

Fig. 6 TRPV2 was palmitoylated at cysteine 277 site and reduced microglial Aβ phagocytosis. Microglia or HEK293T cells were transfected with the TRPV2 pCMV-TRPV2-3FLAG-Neo and pCMV-TRPV2-C277A-3FLAG-Neo plasmids for 48 h, and then treated with CBD for 24 h, FITC-Aβ42 (1 μg/ml) was added to the medium for another 24 h. **(A)** and **(B)** Palmitoylation of TRPV2 and TRPV2-C277A detected by ABE assay in HEK293T cells. Cells transiently expressing FLAG-TRPV2 and TRPV2-C277A were immunoprecipitated with anti-TRPV2 antibody. **(C)** Primary microglia were plated at a density of 5×10^4 in poly-D-lysine-coated wells of 24-well plates containing DMEM supplemented with 10% FBS, immunofluorescence analysis of FITC-Aβ42 was performed after allowing uptake of FITC-Aβ42 for 24 h. **(D)** FITC-Aβ42 uptake index was analyzed using the phagocytosis assay. **(E)** Cytosolic and membrane fractions of BV2 cells were obtained and immunoblotted with the indicated antibodies, and GAPDH and ACE2 were used as cytosolic and membrane markers, respectively. **(F)** Immunofluorescence analysis of microglial TRPV2 were determined. $^{***}p < 0.001$ compared to the control, $^{\#\#}p < 0.01$ and $^{\#\#\#}p < 0.001$ compared to the Aβ group, $^{\$\$\$}p < 0.001$ are compared to the C227A group, as obtained by one-way analysis of variance (ANOVA). Con: DMSO

However, the most pronounced increase in FITC-Aβ42 fluorescence intensity is observed in cells treated with CBD, this effect is inhibited by TRPV2 siRNA or the TRPV2 antagonist tranilast [20]. Moreover, CBD effectively penetrates the blood-brain barrier in human brain endothelial cells through TRPV2 activation [42]. Our findings demonstrated that short-term CBD treatment reduced the expression levels of Tau and Iba1 in the cortex of APP/PS1 mice, but the protein levels of BACE, Tau, and Iba1 were significantly increased upon long-term CBD treatment in the hippocampus and cortex of APP/PS1 mice through TRPV2/Akt signaling pathway. Interestingly, long-term CBD administration upregulated APP protein expression and increased Aβ plaques formation in the cortex and hippocampus of APP/PS1 mice. Phagocytosis pivotal for clearing cellular debris, is regulated by phagocytic receptors. [43, 44]. TRPV2 plays a crucial role in microglial phagocytosis through the PKG/PI3K- and iNOS/NO- dependent signaling pathways,. essential for clearing aggregated proteins, and delaying neuropathology while reducing neurodegeneration [23, 45]. Inflammatory cytokines are implicated in AD development and progression [46, 47]. Microglia activation and proinflammatory cytokine production are contribute to Aβ accumulation [46]. Short-term CBD treatment reduced the mRNA levels of Cr3, GPR34, P2Y6, IL-4, IL-6, IL-1β in the cortex of APP/PS1 mice, long-term CBD treatment upregulated the mRNA levels of Iba1, Trem2, P2Y6, IL-6, TNFα, and IL-1β in the cortex and hippocampus of APP/PS1 mice through the TRPV2 channel. However, the mRNA expression showed little variation with protein, this was believed to be due to the fact that the mRNA do not necessarily reflect protein expression levels, this phenomenon was also evident in other study [48]. TRPV2 activation by NO or oxidative stress may sensitize it through methionine oxidation [24, 25]. This activation promotes the influx of sodium and calcium from the extracellular media and/or endoplasmic reticulum, leading to cell depolarization and subsequent microglial phagocytosis or cytokine production [49].

Post-translational protein modification is vital for regulating ion channel and immune signaling, affecting channel expression on the plasma membrane and their biophysical characteristics [26, 50]. TRPV2 channel sensitivity is finely regulated by dynamic phosphorylation and dephosphorylation processes, with the JAK1-TRPV2 axis contributing to immune regulation [26]. Our study revealed that CBD enhanced TRPV2 responses by the PTPN1 phosphatase at specific molecular sites, namely Y338, Y466, and Y520. Tyrosine phosphorylation not only influences TRPV2's sensitivity to stimuli but also modulates macrophage phagocytosis [26]. Increased tyrosine phosphorylation levels heighten TRPV2 sensitivity, boosting microglial Aβ phagocytosis, controlled by phosphatase dephosphorylation. In macrophages, tyrosine phosphorylation directly affects TRPV2's biophysical properties without altering its membrane expression [26]. Our findings indicated that phosphorylation at Y338 and Y520 reduced TRPV2 expression on the plasma membrane. Previous studies have shown that PKC-related or Src-related pathways phosphorylate TRPV1 channel, influencing their surface expression [51, 52]. Additionally, methionine oxidation or endogenous modulators may influence TRPV2 channel sensitivity independently or synergistically [25]. We also have identified palmitoylation at cysteine 277 in TRPV2, which reduced microglial Aβ phagocytosis. Moreover, it was demonstrated that TRPV2 palmitoylation was dynamically regulated by ZDHHC21. Palmitoylation play a crucial role in regulating protein transport, cellular localization, and stability [27]. Interestingly, our findings indicated that palmitoylation directly affected TRPV2's phagocytic ability without altering its membrane expression. Thus, TRPV2 channel is finely maintained through dynamic phosphorylation/dephosphorylation and palmitoylation/depalmitoylation processes.

The study highlights the contribution of TRPV2 ion channel in microglial Aβ phagocytosis and the underlying mechanisms. We observed predominant expression of TRPV2 in microglia, and noted that CBD activation sensitized TRPV2 channel. Short-term CBD injection (i.p.) significantly decreased chronic neuroinflammation and microglial phagocytic receptors in AD mice, and exhibited neuroprotective effect in neurons. Prolonged CBD treatment induced neuroinflammation and disrupted the expression of microglial phagocytic receptors in APP/PS1 mice. Additionally, we identified tyrosine phosphorylation at Tyr(338), Tyr(466), and Tyr(520) sites, which increased microglial Aβ phagocytosis by enhancing TRPV2 channel sensitivity and its localization. Conversely, TRPV2 was palmitoylated at Cys 277 site and blocking TRPV2 palmitoylation improved microglial Aβ phagocytosis, and TRPV2 palmitoylation was dynamically regulated by ZDHHC21. These findings underscore the opposing effects of tyrosine phosphorylation/dephosphorylation and cysteine palmitoylation/depalmitoylation on microglial Aβ phagocytosis mediated by TRPV2 channel (Fig. 7).

Materials and methods

Key resources were shown in Table 1.

Mice and drug treatment

Male mice of 6-months overexpressing APP and PS1, as well as non-transgenic WT littermates, were obtained from Aniphe Biolaboratory (Nanjing, China). All mice were housed in pathogen-free facilities at the Experiment Animal Center of Northwest Normal University

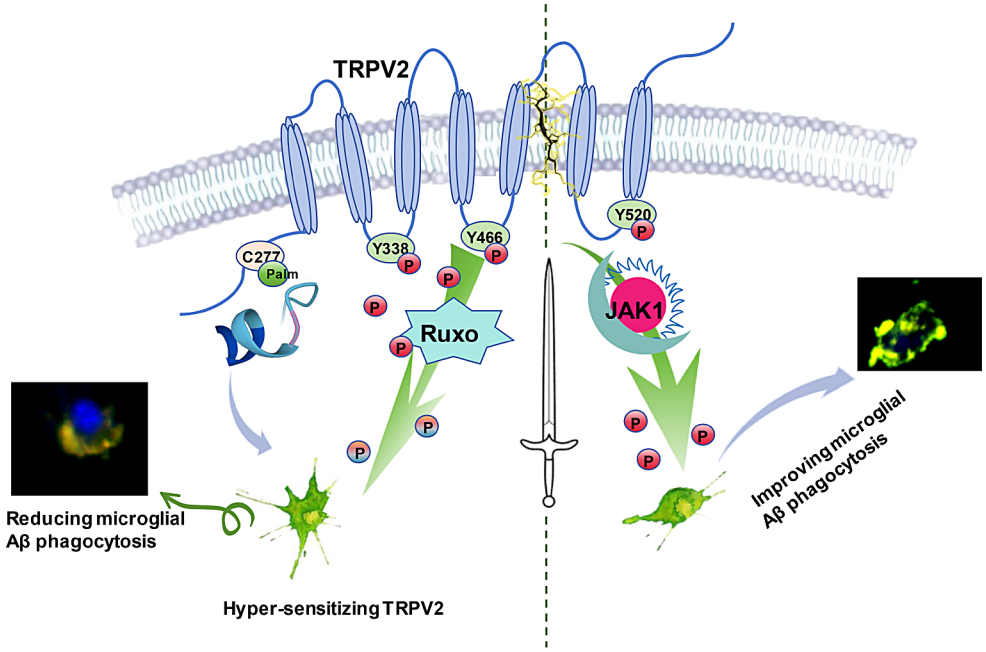

Fig. 7 Tyrosine phosphorylation and palmitoylation of TRPV2 ion channel tuned microglial beta-amyloid peptide phagocytosis. TRPV2 was predominantly expressed in microglia, and CBD could activate and sensitize TRPV2 channel. Short-term CBD injection (i.p.) significantly decreased chronic neuroinflammation and microglial phagocytic receptors in AD mice, and exhibited neuroprotective in neurons. Long-term CBD treatment led to neuroinflammation and impaired the expression of microglial phagocytic receptors in APP/PS1 mice. Furthermore, the hyper-sensitivity of TRPV2 channels was mediated by tyrosine phosphorylation at the Tyr(338), Tyr(466), and Tyr(520) sites, which enhanced microglial Aβ phagocytosis partially dependence on its localization. TRPV2 was palmitoylated at cysteine 277 site and blocking TRPV2 palmitoylation improved microglial Aβ phagocytosis. Moreover, it was demonstrated that TRPV2 palmitoylation was dynamically regulated by ZDHHC21. Microglial TRPV2 channels had contrasting effects on microglial Aβ phagocytosis, and were regulated by tyrosine phosphorylation/dephosphorylation and cysteine palmitoylation/depalmitoylation

with 5–6 mice per cage. Animals were maintained with food and water ad libitum. All experimental procedures were conducted according to the Directive 2010/63/EU of the European Parliament and the Ethical Committee for Human and Animal Experimentation Guidelines at Northwest Normal University. In vivo CBD treatment, 6-month-old APP/PS1 mice or WT mice were administrated intraperitoneally (i.p.) with CBD according to the previous study [20]. The injections continued until mice were euthanized (10 mg/kg per day continued for 1 week (short-term) or 3 weeks (long-term)).

Cell culture

Primary microglia culture was prepared as previously described [23]. Newborn pups were used to isolate primary microglia, which were grown in T-25 flasks in complete DMEM supplemented with 10% FBS, 1% penicillin (70 mg/l), and streptomycin (100 mg/l). The medium was completely replaced every 3 days and achieved after 12 days. The cells were placed on a shaker at 200 rpm for 18 h, the supernatants were collected and centrifuged at 900 g for 4 min. The isolated microglia were resuspended and plated at 5×10^4 cells/cm^2 in different plates. The BV-2 cell line was generously provided by Prof. Shengxiang Zhang from Lanzhou University, while human embryonic kidney (HEK) 293T cells were obtained from ATCC. Both cell lines were cultured in DMEM complete medium and maintained in a 37 °C incubator with 5% CO_2 and 95% humidity. To prepare the CBD solution, it was first dissolved in anhydrous ethyl alcohol and then diluted with serum-free medium.

Western blot and immunoprecipitation assays

Immunoblotting was performed according to previously study [33]. Brain tissues were homogenized, and cells were scraped in ice-cold RIPA protein lysis buffer supplemented with 1% Protease inhibitor cocktail and PMSF. The BCA assay method was used to quantify the concentration. Samples (20 μg) were prepared, subjected to SDS-PAGE, then transferred onto nitrocellulose membranes. The membranes were blocked with 10% nonfat skim milk at room temperature (RT) for 1 h, and incubated overnight at 4 °C with the corresponding primary antibodies. After washing with TBST, the membranes were incubated with the appropriate HRP-conjugated secondary antibodies. Protein bands were visualized using a chemiluminescent HRP substrate and quantified using ImageJ software.

For immunoprecipitation, 1 μg of anti-TRPV2 antibody was conjugated with 25 μl of nanobody manarose beads

Table 1 Key resources were shown

Reagent type (species) or resource	Source	Identifiers
Antibodies		
TRPV2	Alomone Labs (Jerusalem, Israel)	ALO-ACC-032-50
AKT	Proteintech	BS4006
IBA1	Proteintech	10904-1-AP
GAPDH	Proteintech	10494-1-AP
Alexa Flour 594-conjugated Goat Anti-Rabbit IgG (H + L)	Proteintech	SA00013-4
NeuN	Proteintech	26975-1-AP
DYDDDDK tag Recombinant antibody (Binds to FLAG® tag epitope)	Proteintech	80010-1-RR
HRP-conjugated Streptavidin	Proteintech	SA00001-0
phospho-Akt Ser473	Bioworld	9271
CaMKIIα/δ	Bioworld	BS3433
CaMKIIα/δ (phospho-T268)	Bioworld	BS4773
ACE2	Bioss	bs-1004R
Goat Anti-rabbit IgG/HRP	Bioss	bs-0295G
APP/β-Amyloid (NAB228) Mouse mAb	Cell Signaling TECHNOLOGY	2450
BACE	Cell Signaling TECHNOLOGY	5606
Tau	Cell Signaling TECHNOLOGY	4019
Anti-mouse IgG, HRP-linked Antibody	Cell Signaling TECHNOLOGY	7076
β-Amyloid(D54D2)XP®Rabbit mAb	Cell Signaling TECHNOLOGY	8243
Chemical compound, drug		
cannabidiol	Refines Biotechnology	13956-29-1
PTP Inhibitor I	AbMole BioScience	M20414
PTP Inhibitor II	AbMole BioScience	M20410
INCB18424 (Ruxo)	AbMole BioScience	M1787
BMCC-Biotin	Thermo scientific	XF344410
2-Bromohexadecanoic acid	Merck	18263-25-7
Aβ (1–42)	GL Biochem	052487
Fitc-Aβ (1–42)	GL Biochem	250,857
Other reagents/kits		
Glycine	BioFROxx	1275GR500
SDS	BioFROxx	3250KG001
Cryo Embedding Medium	Biosharp	B2557A
Membrance and cytoplasmic Extraction kit	Biosharp	BL671A
Anti-FLAG Nanobody Magarose beads	AlpaLifeBio	KTSM1338
BeyoMay™ protein Atg Magnetic Beads	Beyotime	P2108
Protein A/G Magnetic Beads	MCE	HY-K0202
Protease inhibitor cocktail	MCE	HY-K0010
MTT	MCE	298-93-1
Serum-free cell Cryopreservation Medium	Cellor Lab	BY002P
Lipofectamine 2000	Invitrogen	2,536,760
Revertflid First strand cDNA synthesis kit	Thermo scientific	91,279,588
GeneJET RNA Purification kit	Thermo scientific	K0731
Taq SYBR® Green qPCR Premix	Labead	R0202-02
E.Z.N.A.®Endo-Free plasmid Midi kit	Omega	D6915030000L02v038
Ammonium persulfate	Tianjin Damao chemical reagent factory	7727-54-0
paraformaldehyde	Tianjin Damao chemical reagent factory	30525-89-4
sugar	Beichen Founder reagent factory	/
Sodium chloride	Beichen Founder reagent factory	/
Anhydrous sodium dihydrogen phosphate	Sinopharm Group Chemical reagent Co., LTD	7558-80-7
Anhydrous disodium hydrogen phosphate	Sinopharm Group Chemical reagent Co., LTD	7558-79-4
Tricolor Prestained Protein Marker	epizyme	WJ103
carbinol	Yantai Shuangshuang Chemical Co., LTD	/
Isopropyl alcohol	Yantai Shuangshuang Chemical Co., LTD	/

Table 1 (continued)

Reagent type (species) or resource	Source	Identifiers
Ethyl alcohol	Yantai Shuangshuang Chemical Co., LTD	/
xylene	Yantai Shuangshuang Chemical Co., LTD	/
N.N.N.n-tetramethylenediamine	Yantai Shuangshuang Chemical Co., LTD	/
chloroform	Yantai Shuangshuang Chemical Co., LTD	/
Tween-20	Solarbio	T8220
Triton x-100	Solarbio	T8200
Hydroxylamme solution	Solarbio	7803-49-8
BCA Protein Assay Kit	Solarbio	PC0020
β-Mercaptoethanol	Solarbio	M8210
Normal Goat Serum	Solarbio	SL038
Glycero	Solarbio	G8190
Antigen Retrieval Solution, 1x	Solarbio	C1035
Bromphenol Blue	Solarbio	115-39-9
PMSF (100mM)	Solarbio	P0100-01
DNase/RNase-Free water	Solarbio	R1600
0.01 M PBS (powder, pH7.2-7.4)	Solarbio	P1010
LB broth, powder	Solarbio	L1010
LB agar, powder	Solarbio	L1015
Ampicillin	Solarbio	A6920
Kanamycin Sulfate	Solarbio	K8020
Mounting Medium, antifading	Solarbio	S2100
M5 Total RNA Extraction Reagent	Solarbio	MF034-01
DMSO	Solarbio	D8371
Polylysine, 10x	Solarbio	P2100
RNA extract	Solarbio	P1025
NP-40 lysisi buffer	Solarbio	N8032
Hypersensitive ECL kit	Proandy	10,144
WB and IP cell lysate	Beyotime	P0013J
Hydroxylamine solution	Sigma Aldrich Trading Co., LTD	7803-49-8
2-Bromohexadecanoic acid	Sigma Aldrich Trading Co., LTD	18263-25-7
Sodium chloride injection	Sichuan Kelun Pharmaceutical Co., Ltd.	N23040605
Pentobarbital sodium	Shanghai Zhongqin Chemical Reagent Co., LTD	/
High protein skim high calcium milk powder	Erie	/
Rabbit IgG - Immunohistochemical kit	Bosyer Bio	SA1022

or protein A/G magnetic beads at 4 °C for 1 h on a shaking platform. The conjugated beads were washed three times with lysis buffer. They were incubated with 0.2 mg of precleared tissues or cell lysates and left overnight at 4 °C. Following another set of washes, the resulting precipitants were resuspended in 2 × SDS sample buffer, boiled, and subjected to SDS-PAGE. Finally, immunoblot analysis was conducted using the appropriate antibodies.

Immunohistochemistry

Following CBD or saline injection, both the APP/PS1 and WT mice were perfused with ice-cold heparinized saline and 4% paraformaldehyde in 0.1 M PBS at pH 7.4. Brains were collected and fixed for 72 h at 4 °C. To facilitate dehydration, brains were treated with sucrose solution (10%, 20%, and 30%) and then embedded in O.C.T. compound. Coronal Sect. (10 μm) were prepared using a freezing microtome. Endogenous peroxidases were inhibited with 3% H_2O_2, and sections were blocked for 1.5 h with 5% goat serum containing 0.3% Triton X-100 before overnight incubation with primary antibodies at 4 °C. Detection was performed using SABC-POD and DAB kits and images were captured using a light microscope (Leica, Germany). Quantitative analysis was performed using ImageJ, and determined the number of Aβ plaques and NeuN levels in the prefrontal cortex (PFC) and hippocampal DG region. Three slices per mouse and five mice per group were sampled, average data were used to represent the data for each mouse.

Preparation of amyloid-beta

The preparation of amyloid-beta was adapted from a previous study [33]. Amyloid peptides (1–42) were dissolved in 20 μl of DMSO and vigorously mixed for 5 min on a shaker. Next, 424 μl of PBS was added to the solution to achieve a final concentration of 500 μM. The solution

was then incubated at 37 °C for 24 h, it was centrifuged at 14,000 g for 10 min at 4 °C. The resulting supernatant, containing soluble Aβ1–42 oligomers, was collected for further use.

Immunocytochemistry

Cells were cultured on poly-D-lysine coated coverslips in 24-well plates. Following treatment, cells were fixed with 2% paraformaldehyde for 20 min, followed by triple washes with PBS for 5 min each. After permeabilized with 1% Triton X-100 for 7 min and blocked using 10% normal goat serum for 1 h, Subsequently, cells were subjected to overnight incubation at 4 °C with antibodies (1:200). After three washes with PBS at RT. A fluorescent goat anti-rabbit secondary antibody labeled with Alexa Fluor 594 (1:400) were incubated for 90 min. The cells were stained with Hoechst 33,258 and coverslips were mounted onto microscope slides using Fluoromount-G. Immunofluorescence sections were captured using fluorescence microscope (Leica, Germany) at 20 × and 40 × magnifications. Image processing and analysis were performed using ImageJ, and immunofluorescence density was quantified across at least five selected images.

Quantitative reverse transcription (qRT) PCR

RNA was extracted from brain tissues using either the RNeasy Mini Kit or TRIzol, following the manufacturer's instructions. The quantity and quality of the purified RNAs were assessed using NanoDrop 2000 UV-Vis Spectrophotometer (Thermo Scientific). Subsequently, cDNA synthesis was performed using the RevertAid First Strand cDNA Synthesis Kit. The synthesized cDNA was then amplified in a 20 µl PCR reaction using SYBR green PCR master mix (TIANGEN, # FP205). Primer pairs listed in Table 2 were used for amplification. Gene expression was analyzed using a real-time detection system (Thermo Scientific) using 96-well plates in a total reaction volume of 20 µl. The expression levels of the target genes were normalized to GAPDH expression in the same sample, and quantified using the $2^{-\Delta\Delta Ct}$ method.

Table 2 Primers and their sequences for fluorescence quantitative PCR

Primer	sequence
TRPV2 Forward	GGTATGGGTGAGCTGGCTTTT
TRPV2 Reverse	AGGACGTAGGTGAGGAGGAC
TREM2 Forward	CTGATCACAGCCCTGTCCCAA
TREM2 Reverse	CGTCTCCCCCAGTGCTTCAA
Gpr34 Forward	CTTCAGGAAAGCTTCAACTC
Gpr34 Reverse	GTAACTATCAGGAGGAGAGC
P2Y6 Forward	GTGAGGATTTCAAGCGACTGC
P2Y6 Reverse	TCCCCTCTGGCGTAGTTATAGA
IL-4 Forward	GGTCTCAACCCCCAGCTAGT
IL-4 Reverse	GCCGATGATCTCTCTCAAGTGAT
Iba1 Forward	ATCAACAAGCAATTCCTCGATGA
Iba1 Reverse	CAGCATTCGCTTCAAGGACATA
Cr3 Forward	AATTGAGGGCACGCAGACA
Cr3 Reverse	GCCCAGCAAGGGACCATTAG
TNFα Forward	ACTCCAGGCGGTGCCTATGT
TNFα Reverse	GTGAGGGTCTGGGCCATAGAA
IL-1β Forward	TCCAGGATGAGGACATGAGCAC
IL-1β Reverse	GAACGTCACACACCAGCAGGTTA
IL-6 Forward	CCACTTCACAAGTCGGAGGCTTA
IL-6 Reverse	CCAGTTTGGTAGCATCCATCATTTC
GAPDH Forward	TGTGTCCGTCGTGGATCTGA
GAPDH Reverse	TTGCTGTTGAAGTCGCAGGAG

Phagocytosis assays

The phagocytosis of aggregated Aβ1–42 was analyzed according to previously study [20]. In brief, FITC-Aβ1–42 was allowed to aggregate for 24 h at 37 °C. Microglia were seeded at a density of 2×10^4 cells per well in 96-well plates and incubated overnight. After treatment, the culture media was removed, and the cells were washed twice with fresh complete DMEM remove any extracellular Aβ. Finally, the plate was protected from light, and the fluorescence intensity was measured at 485-nm excitation/538-nm emission using a multifunctional microplate reader. Results are expressed as the percentage of fold-change in fluorescence intensity compared to control samples.

Cell survival and apoptosis assay

Cell viability was evaluated using the 3-[4,5-dimethylthiazol-2-yl]2,5-diphenyltetrazolium bromide salt (MTT) reduction assay. Cells were treated with MTT and incubated for 4 h. After removing the culture medium, DMSO was added to dissolve the formazan crystals. The absorbance at 490 nm was measured using a multifunctional microplate reader. To quantify apoptosis, primary neurons were fixed in 2% paraformaldehyde and stained with 1 µg/ml of the DNA dye Hoechst 33,342. Apoptotic cells, characterized by fragmented or condensed nuclei, were observed under a fluorescence microscope, while cells showing uniformly stained nuclei were scored as viable. At least 300 neurons from 6 randomly selected fields per well were counted for quantification.

Plasmid construction, and transfection

For plasmid construction and transfection, mouse TRPV2 cDNA sequences were mutated into the pCMV-3×FLAG-Neo vector (MIAOLING BIOLOGY, Wuhan, China). Various plasmids, including pCMV-TRPV2-Y338F-3FLAG-Neo (# G20943), pCMV-TRPV2-Y466F-3FLAG-Neo (# G20944), pCMV-TRPV2-Y520F-3FLAG-Neo (# G20945), pCMV-TRPV2-Y338/466/520F-3FLAG-Neo (# G20946), pCMV-TRPV2-C277A-3FLAG-Neo, pCMV-TRPV2-3FLAG-Neo and pCMV-HA-ZDHHC21-Neo employed. Briefly, BV2 or HEK293T cells were seeded at densities of 2.0×10^5 cells per well in a 6-well plate, 5.0×10^4 cells per well in a 24-well plate, and 1.0×10^4 cells

per well in a 96-well plate. Transfection was conducted with 2 μg of DNA, diluted in 1800 μl–450 μl of fresh DEME, and incubated for 5 min, and followed by the addition of 4 μl Lipofectamine 2000. After a 20-min incubation, the mixture was added to the cells and incubated 4 h, subsequently, the medium was replaced, and the cells were cultured for 48 h. Tyrosine phosphorylation analysis of TRPV2 was performed using immunoblotting, immunocytochemistry, or phagocytosis assays following established protocols.

Acyl-biotin exchange (ABE) assay

The ABE assay was conducted following the previous study [34]. Briefly, cells transfected with pCMV-TRPV2-3FLAG-Neo plasmid and pCMV-TRPV2-C277A-3FLAG-Neo were harvested 48 h post-transfection and rinsed with cold PBS. Prior to lysing cells or brain tissue, a solution of 50 mM N-ethylmaleimide (NEM; Sangon Biotech, A600450) in ethanol was freshly added to lysis buffer (50 mM Tris-HCl, pH 7.5; 150 mM NaCl; 1 mM $MgCl_2$; 1% NP-40; and 10% glycerol) with inhibitor cocktail. The cell and brain tissue lysates were then suspended in the lysis buffer containing NEM and incubated at 4 °C for 1.5 h, followed by centrifugation at 15,000 rpm for 30 min at 4 °C. The supernatants were incubated overnight with both anti-Flag antibody (GenScript, 80010-1-RR) or HA-tag (Santa Cruz Biotechnology, sc-7392) and protein A/G magnetic beads (MedChemExpress, HY-K0202). After incubation, the beads underwent five washes with lysis buffer (pH 7.5) followed by three washes with lysis buffer (pH 7.2). For hydroxylamine (HAM; MACKLIN, H828371) treatment, the beads were divided into two equal tubes (+HAM and -HAM). The +HAM tube received freshly prepared lysis buffer (50 mM Tris-HCl, pH 7.2; 150 mM NaCl; 1 mM $MgCl_2$; 1% NP-40; 10% glycerol; 0.75 M HAM; and inhibitor cocktail) and was incubated at RT for 1 h. The HAM tube served as a control and received lysis buffer at pH 7.2. The beads were washed four times with lysis buffer (pH 7.2) and then three washes with lysis buffer (pH 6.2). Subsequently, the beads were treated with 5 μM biotin-BMCC (Sangon Biotech, C1002225) in freshly prepared lysis buffer (pH 6.2) and incubated for 1 h at 4 °C. The immunoprecipitated samples were detected using western blotting with HRP-conjugated streptavidin (Beyotime, SA00001-0) and anti-Flag or -HA antibody.

Membrane and cytosol preparation

Membrane and cytosol preparation was assessed using a slightly modified membrane assay. Plasmids were transfected into BV2 cells for 48 h. Approximately 1×10^7 cells were harvested and washed twice with cold PBS (1, 000 g each time, 5 min). Then cells were treated with 1 ml of lysis buffer (1 ml lysis buffer+1 μl DTT+1 μl protease inhibitor) to each sample, followed by freezing in liquid nitrogen and thawing at 37 °C. The cells were vortexed for 30 s and placed on ice for five cycles of 1 min each. The samples were centrifuged at 14,000 g for 10 min at 4 °C, and the supernatant was the cytoplasm. The membrane fraction was isolated by centrifugation at 15,000 rpm for 20 min at 4 °C.

Model building and bioinformatics analysis

The conformance of TRPV2 sequences in mice was predicted using the website https://www.ebi.ac.uk/Tools/msa/clustalo/. IBS software was used to map different regions of TRPV2. AlphaFold2 was used to mark the binding sites of TRPV2 (TRPV2-MOUSE, # Q9WTR1) to CBD and analyzed by VMD software. For TRPV2 gene expression analysis, the Z-score of cell-type specific data from healthy human brain cortical tissue for each gene across samples was utilized, as shown in previous study, the score of τ is ≥0.8, the gene was selected for further analysis [32].

Statistical analysis

The data are presented as means±standard errors and analyzed using GraphPad software (GraphPad Software Inc., La Jolla, CA, USA) and SPSS software (SPSS Inc., Chicago, IL, USA). The statistical significance of the difference between two groups was determined using the unpaired, two-tailed Student's *t*-test analysis. For comparison involving multiple groups, one-way ANOVA followed by Post hoc Tukey's test was applied. Data points that deviated more than two standard deviations from the mean were identified as significant outliers and were excluded from further analysis. Statistical significance levels of $p<0.05$, $p<0.01$, and $p<0.001$ are indicated in the figures.

Abbreviations

ABE	Acyl-biotin exchange
AD	Alzheime's disease
Aβ	Amyloid –β
Akt	Protein kinase B
2-BP	2-Bromopalmitate
CBD	Cannabidiol
CNS	Central nervous system
CR3	Complement receptor 3
DG	Dentate gyrus
DMEM	Dulbecco's modified Eagle's medium
ECL	Chemiluminescence
FBS	Fetal bovine serum
GAPDH	Glyceraldehyde 3-phosphate dehydrogenase
GPR34	G protein–coupled receptor 34
HEK	Human embryonic kidney
IGF-1	Insulin-like growth factor-1
i.p	Intraperitoneally
IL-6	Interleukin-6
IL-1β	Interleukin-1β
MCI	Mild cognitive impairment
MTT	3-[4,5-dimethylthiazol-2-yl]2,5-diphenyltetrazolium bromide salt
NEM	N-ethylmaleimide
NORT	Novel object recognition task

OGD	Oxygen-glucose deprivation
P2Y6	Pyrimidinergic receptor
PBS	Phosphate-buffered saline
PFC	Prefrontal cortex
PI3K	Phosphoinositide 3-kinase
PTPN1	Protein tyrosine phosphatase non-receptor type 1
qRT-PCR	Quantitative realtime polymerase chain reaction
TBST	Tris-buffered saline-Tween
TNFα	Tumor necrosis factor α
Trem2	Triggering receptor expressed on myeloid cells
T2DM	Type 2 diabetes mellitus
TRPV2	Transient receptor potential vanilloid family type 2

Supplementary Information

The online version contains supplementary material available at https://doi.org/10.1186/s12974-024-03204-6.

Supplementary Material 1

Supplementary Material 2

Acknowledgements
This work was funded by the National Nature Science Foundation of China (Grant no. 32360219 and no. 32160210.); Natural Science Foundation of Gansu Province (Grant no.21JR7RA137); Youth Talents Lifting Project Foundation of Northwest Normal University (NWNU-LKQN2021-01).

Author contributions
The conception and design of the work were prepared by Yang S. The experiment was performed by Du Y, Zhao XQ, Tang Q, and Li Y, while the analysis and interpretation of data were done by Du Y and Zhang Y. Drafting of the manuscript was done by Yang S. All the authors revised the manuscript and approved the submission.

Data availability
No datasets were generated or analysed during the current study.

Declarations

Ethics approval and consent to participate
Approved by Ethical Committee for Human and Animal Experimentation Guidelines at Northwest Normal University.

Consent for publication
Not applicable.

Competing interests
The authors declare no competing interests.

Received: 11 April 2024 / Accepted: 13 August 2024
Published online: 03 September 2024

References

1. Jucker M, Walker LC. Alzheimer's disease: from immunotherapy to immunoprevention. Cell. 2023;186:4260–70.
2. Verkhratsky A, Zorec R, Rodríguez JJ, et al. Astroglia dynamics in ageing and Alzheimer's disease. Curr Opin Pharmacol. 2016;26:74–9.
3. GBD 2019 Dementia Forecasting Collaborators. Estimation of the global prevalence of dementia in 2019 and forecasted prevalence in 2050: an analysis for the global burden of Disease Study 2019. Lancet Public Health. 2022;7:e105–25.
4. Querfurth HW, LaFerla FM. Alzheimer's disease. N Engl J Med. 2010;362:329–44.
5. Scheltens P, Blennow K, Breteler MM, et al. Alzheimer's disease. Lancet. 2016;388:505–17.
6. Wang J, Gu BJ, Masters CL, et al. A systemic view of Alzheimer disease - insights from amyloid-β metabolism beyond the brain. Nat Rev Neurol. 2017;13:612–23.
7. Huang Y, Happonen KE, Burrola PG, et al. Microglia use TAM receptors to detect and engulf amyloid β plaques. Nat Immunol. 2021;22:586–94.
8. Zhou Y, Song WM, Andhey PS, et al. Human and mouse single-nucleus transcriptomics reveal TREM2-dependent and TREM2-independent cellular responses in Alzheimer's disease. Nat Med. 2020;26:131–42.
9. Tang R, Liu H. Identification of temporal characteristic networks of peripheral blood changes in Alzheimer's Disease based on weighted gene co-expression network analysis. Front Aging Neurosci. 2019;11:83.
10. Entin-Meer M, Cohen L, Hertzberg-Bigelman E, et al. TRPV2 knockout mice demonstrate an improved cardiac performance following myocardial infarction due to attenuated activity of peri-infarct macrophages. PLoS ONE. 2017;12:e0177132.
11. Lévêque M, Penna A, Le Trionnaire S, et al. Phagocytosis depends on TRPV2-mediated calcium influx and requires TRPV2 in lipids rafts: alteration in macrophages from patients with cystic fibrosis. Sci Rep. 2018;8:4310.
12. Shibasaki K, Murayama N, Ono K, et al. TRPV2 enhances axon outgrowth through its activation by membrane stretch in developing sensory and motor neurons. J Neurosci. 2010;30:4601–12.
13. Santoni G, Farfariello V, Liberati S, et al. The role of transient receptor potential vanilloid type-2 ion channels in innate and adaptive immune responses. Front Immunol. 2013;4:34.
14. Su N, Zhen W, Zhang H, et al. Structural mechanisms of TRPV2 modulation by endogenous and exogenous ligands. Nat Chem Biol. 2023;19:72–80.
15. Coles M, Watt G, Kreilaus F, et al. Medium-dose chronic cannabidiol treatment reverses object recognition memory deficits of APP swe /PS1ΔE9 transgenic female mice. Front Pharmacol. 2020;11:587604.
16. Hao FJ, Feng YQ. Cannabidiol (CBD) enhanced the hippocampal immune response and autophagy of APP/PS1 Alzheimer's mice uncovered by RNA-seq. Life Sci. 2021;264:118624.
17. Wang ZZ, Zheng P, Chen X et al. Cannabidiol induces autophagy and improves neuronal health associated with SIRT1 mediated longevity.Geroscience. 2022;44:1505–24.
18. Gochman A, Tan XF, Bae C, et al. Cannabidiol sensitizes TRPV2 channels to activation by 2-APB. Elife. 2023;12:e86166.
19. Pumroy RA, Samanta A, Liu Y, et al. Molecular mechanism of TRPV2 channel modulation by cannabidiol. Elife. 2019;8:e48792.
20. Yang S, Du Y, Zhao X, et al. Cannabidiol enhances microglial Beta-amyloid peptide phagocytosis and clearance via Vanilloid Family Type 2 Channel activation. Int J Mol Sci. 2022;23:5367.
21. Lana D, Landucci E, Mazzantini C, et al. The Protective Effect of CBD in a model of in Vitro Ischemia May be mediated by Agonism on TRPV2 Channel and Microglia activation. Int J Mol Sci. 2022;23:12144.
22. Hu J, Gao Y, Huang Q, et al. Flotillin-1 interacts with and sustains the surface levels of TRPV2 Channel. Front Cell Dev Biol. 2021;9:634160.
23. Maksoud MJE, Tellios V, An D, et al. Nitric oxide upregulates microglia phagocytosis and increases transient receptor potential vanilloid type 2 channel expression on the plasma membrane. Glia. 2019;67:2294–311.
24. Maksoud MJE, Tellios V, Lu WY. Nitric oxide attenuates microglia proliferation by sequentially facilitating calcium influx through TRPV2 channels, activating NFATC2, and increasing p21 transcription. Cell Cycle. 2021;20:417–33.
25. Fricke TC, Echtermeyer F, Zielke J, et al. Oxidation of methionine residues activates the high-threshold heat-sensitive ion channel TRPV2. Proc Natl Acad Sci U S A. 2019;116:24359–65.
26. Mo X, Pang P, Wang Y, et al. Tyrosine phosphorylation tunes chemical and thermal sensitivity of TRPV2 ion channel. Elife. 2022;11:e78301.
27. Ernst AM, Syed SA, Zaki O, et al. S-Palmitoylation Sorts Membrane Cargo for Anterograde Transport in the Golgi. Dev Cell. 2018;47:479–e493477.
28. Yuan W, Lu L, Rao M, et al. GFAP hyperpalmitoylation exacerbates astrogliosis and neurodegenerative pathology in PPT1-deficient mice. Proc Natl Acad Sci U S A. 2021;118:e2022261118.
29. Gao X, Kuo CW, Main A, et al. Palmitoylation regulates cellular distribution of and transmembrane ca flux through TrpM7. Cell Calcium. 2022;106:102639.
30. Chandra M, Zhou H, Li Q, et al. A role for the Ca2 + channel TRPML1 in gastric acid secretion, based on analysis of knockout mice. Gastroenterol Gastroenterol. 2011;140:857–67.
31. Hong C, Choi SH, Kwak M, et al. TRPC5 channel instability induced by depalmitoylation protects striatal neurons against oxidative stress in Huntington's disease. Biochim Biophys Acta Mol Cell Res. 2020;1867:118620.

32. Galea E, Weinstock LD, Larramona-Arcas R, et al. Multi-transcriptomic analysis points to early organelle dysfunction in human astrocytes in Alzheimer's disease. Neurobiol Dis. 2022;166:105655.
33. Yang S, Pascual-Guiral S, Ponce R, et al. Reducing the levels of akt activation by PDK1 knock-in mutation protects neuronal cultures against Synthetic amyloid-Beta peptides. Front Aging Neurosci. 2018;9:435.
34. Huang X, Yao J, Liu L, et al. S-acylation of p62 promotes p62 droplet recruitment into autophagosomes in mammalian autophagy. Mol Cell. 2023;83:3485–e35013411.
35. Mukai K, Konno H, Akiba T, et al. Activation of STING requires palmitoylation at the Golgi. Nat Commun. 2016;7:11932.
36. Bluhm Y, Raudszus R, Wagner A, et al. Valdecoxib blocks rat TRPV2 channels. Eur J Pharmacol. 2022;915:174702.
37. Aso E, Palomer E, Juvés S, et al. CB1 agonist ACEA protects neurons and reduces the cognitive impairment of AβPP/PS1 mice. J Alzheimers Dis. 2012;30:439–59.
38. Martín-Moreno AM, Brera B, Spuch C, et al. Prolonged oral cannabinoid administration prevents neuroinflammation, lowers β-amyloid levels and improves cognitive performance in tg APP 2576 mice. J Neuroinflammation. 2012;9:8.
39. Karl T, Garner B, Cheng D. The therapeutic potential of the phytocannabinoid cannabidiol for Alzheimer's disease. Behav Pharmacol. 2017;28:142–60.
40. Pumroy RA, Protopopova AD, Fricke TC, et al. Structural insights into TRPV2 activation by small molecules. Nat Commun. 2022;13:2334.
41. Zhang L, Simonsen C, Zimova L, et al. Cannabinoid non-cannabidiol site modulation of TRPV2 structure and function. Nat Commun. 2022;13:7483.
42. Luo H, Rossi E, Saubamea B, et al. Cannabidiol increases Proliferation, Migration, Tubulogenesis, and Integrity of Human Brain endothelial cells through TRPV2 activation. Mol Pharm. 2019;16:1312–26.
43. Jiang T, Tan L, Zhu XC, et al. Upregulation of TREM2 ameliorates neuropathology and rescues spatial cognitive impairment in a transgenic mouse model of Alzheimer's disease. Neuropsychopharmacology. 2014;39:2949–62.
44. Lee CYD, Daggett A, Gu X, et al. Elevated TREM2 gene dosage reprograms Microglia Responsivity and ameliorates pathological phenotypes in Alzheimer's Disease models. Neuron. 2018;97:1032–e10481035.
45. Lucin KM, O'Brien CE, Bieri G, et al. Microglial beclin 1 regulates retromer trafficking and phagocytosis and is impaired in Alzheimer's disease. Neuron. 2013;79:873–86.
46. Wang WY, Tan MS, Yu JT, et al. Role of pro-inflammatory cytokines released from microglia in Alzheimer's disease. Ann Transl Med. 2015;3:136.
47. Sipe GO, Lowery RL, Tremblay M, et al. Microglial P2Y12 is necessary for synaptic plasticity in mouse visual cortex. Nat Commun. 2016;7:10905.
48. Kleinridders A, Ferris HA, Reyzer ML et al. Regional differences in brain glucose metabolism determined by imaging mass spectrometry.Mol Metab. 2018;12:113–21.
49. Enrich-Bengoa J, Manich G, Valente T, et al. TRPV2: a Key Player in Myelination disorders of the Central Nervous System. Int J Mol Sci. 2022;23:3617.
50. Agarwal N, Taberner FJ, Rangel Rojas D, et al. SUMOylation of enzymes and Ion channels in sensory neurons protects against metabolic dysfunction, Neuropathy, and sensory loss in diabetes. Neuron. 2020;107:1141–e11591147.
51. Studer M, McNaughton PA. Modulation of single-channel properties of TRPV1 by phosphorylation. J Physiol. 2010;588:3743–56.
52. Zhang X, Huang J, McNaughton PA. NGF rapidly increases membrane expression of TRPV1 heat-gated ion channels. Embo j. 2005;24:4211–23.

Publisher's note